Optimal jumping strategies from compliant surfaces: A simple model of springboard standing jumps

Kuangyou B. Cheng, Mont Hubbard *

Sports Biomechanics Laboratory, Department of Mechanical and Aeronautical Engineering, University of California, Davis, CA 95616, USA

Abstract

A simple model of standing dives is used to investigate optimal jumping strategies from compliant surfaces and applied to springboard diving. The human model consists of a massless leg actuated by knee torque, and a lumped torso mass centered above the leg. The springboard is modeled as a mass-spring system. Maximum jump height for a male and a female is calculated by controlling knee-torque activation level as a function of time. The optimization includes constraints on minimum and maximum knee angle, rate of change of normalized activation level, and contact duration. Simulation results for maximal springboard depression and diver takeoff velocity agree reasonably with experimental data, even though larger board tip velocities are necessarily predicted earlier during the contact period. Qualitatively similar multiple pulse knee-torque activation patterns are found over various conditions and are different from those in rigid-surface jumping. The model is less able to predict accurately jump height at high fulcrum number since jumpers may have difficulty behaving optimally at non-preferred fulcrum settings. If strength is proportional to the product of mass and leg length, increasing leg length is more effective in increasing jump height than is increasing mass.
© 2004 Published by Elsevier B.V.

---

* Corresponding author. Tel.: +1-530-752-6450; fax: +1-530-752-4158.
E-mail address: mhubbard@ucdavis.edu (M. Hubbard).

1. Introduction

Although many studies have investigated maximal jumping strategies, virtually all have considered jumps from rigid surfaces. Mathematical models of increasing complexity have been used to comprehend strategies for maximizing standing jump height (Levine, Christodoulou, & Zajac, 1983; Levine, Zajac, Belzer, & Zomlefer, 1983; Pandy, Zajac, Sim, & Levine, 1990; van Soest, Schwab, Bobbert, & van Ingen Schenau, 1993) from a rigid surface. Numerous experimental studies (e.g. Bobbert & van Ingen Schenau, 1988) have measured ground reaction forces, muscle EMG, and joint kinematics. Other work (Alexander, 1990; Seyfarth, Blickhan, & van Leeuwen, 2000; Seyfarth, Friedrichs, Wank, & Blickhan, 1999) used extremely simple dynamic models to understand optimal running high- and long-jumping strategies. However, except for considering the effect of surface stiffness on leg stiffness (Ferris & Farley, 1997) and on running speed (McMahon, 1978; McMahon & Greene, 1979), no systematic study exists concerning surface compliance effects on maximum-effort jumping.

This is curious since several athletic activities (e.g. springboard diving and gymnastics) involve maximal jumping from surfaces with substantial compliance. Diving springboard stiffness can be adjusted using fulcrum settings between 1 (stiffest) and 9 (softest). In springboard diving competitions divers need to perform both running and standing dives. In the former, divers approach the board tip, execute a hurdle jump, and recatch the board for takeoff. In standing dives, however, divers begin at the tip, and maintain contact with the board until takeoff.

Rather than studying how optimal jumping strategies are affected by surface compliance, most springboard diving studies have addressed running dive kinematics, including vertical velocity (Miller & Munro, 1984, 1985) and angular momentum (Sanders & Wilson, 1987; Miller & Sprigings, 2001). Other work concerned springboard kinetics (Miller, 1983) and modeling with linear or rotational mass-spring systems (Kooi & Kuipers, 1994; Sprigings, Stilling, & Watson, 1989, 1990). Springboard tip kinematics were investigated (Jones & Miller, 1996; Jones, Pizzimenti, & Miller, 1993; Miller, Osborne, & Jones, 1998). Sprigings and Watson (1983) investigated the arms' role in vertical velocity production using a simple model neglecting leg action. Boda (1993) identified optimal standing dive fulcrum settings using regression analysis.

Although running dive kinematics are reasonably well understood, neither kinematic features nor coordination strategies of compliant-surface jumping (nor springboard standing jumps) have been described in detail. Validity of a mass-spring springboard model has been established, but diver–board force interaction and optimal fulcrum setting in standing dives are not completely understood. This study's purpose is to use a simple model to investigate optimal strategies (joint torque activation patterns) in compliant-surface jumping using springboard diving for experimental comparison. We try to understand whether general coordination patterns exist for maximizing jump height different from those in rigid-surface jumping. Furthermore, since divers may be biased toward a preferred fulcrum setting (due to lack of practice at other settings), simulation is necessary for testing

whether jump height is affected by fulcrum setting with the best setting differing among divers.

2. Methods

The human model is a two-link system with massless legs and lumped body mass, mechanically identical to that Alexander (1990) used to study rigid-surface jumping. The surface (springboard) is modeled by a mass-spring system (Fig. 1a). Frictionless revolute knee joint rotation is driven by a torque generator. Trunk and arm movements are important for gaining angular momentum, and their role in vertical velocity production has been investigated using a simple model without legs (Sprigings & Watson, 1983). Nevertheless, angular trunk and arm motions are neglected because our focus is on understanding maximizing jump height using the simplest possible model, and because this model has led to reasonable results (Alexander, 1990; Challis, 1998; Seyfarth et al., 2000). Jumper horizontal velocity is neglected.

The springboard modeled is a Maxiflex "B" springboard (Fig. 1b). Although a rotational mass-spring system has been proposed (Kooi & Kuipers, 1994), we chose a translational mass-spring model due to the human model's one-dimensional (1-D) characteristics. Stiffness k and equivalent board mass m_b for fulcrum settings $S = 1$, 5, and 9 were measured by Sprigings et al. (1990) and interpreted by Miller et al. (1998). Cubic splines interpolate m_b and k at other settings (Table 1). To investigate
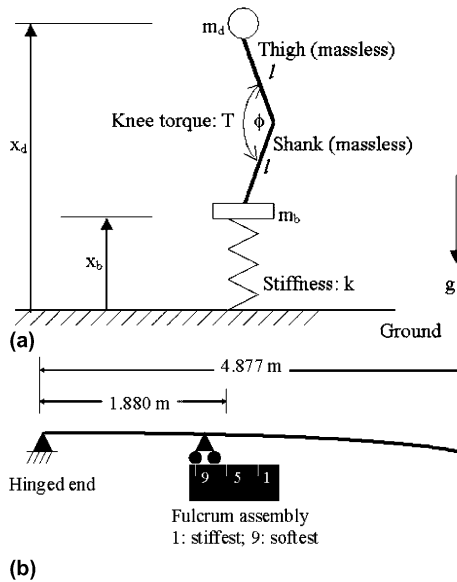
Fig. 1. (a) Dynamic 2-DOF model consists of two masses connected by massless legs and supported on compliant surface. (b) The stiffness of a diving springboard can be adjusted by changing the fulcrum position between 1 and 9. The distance between consecutive numbers is 0.073 m.

Table 1
Equivalent board mass and stiffness dependence on fulcrum number

Fulcrum	1	3	5	7	9
m_b (kg)	6.6	6.95	7.3	7.65	8.0
k (N/m)	6400	6200	5900	5500	5000

the sensitivity of jump height and torque activation patterns to mass and leg length, calculations are done for several mass/length jumper parameters.

Knee angle changes generally involve length changes of contractile and series elastic components of extensor muscles. Although we first performed simulations with and without series elastic compliance, surprisingly very little difference was found in terms of jump height and knee-torque patterns. Seyfarth et al. (2000) also found that rigid-surface jumping height was not sensitive to it. Thus we neglect series elastic compliance in the following calculations. Knee torque is assumed to be the product of maximum torque T_{max} and three factors: angle dependence $f(\phi)$, angular velocity dependence $h(\dot{\phi})$, and effective muscular activation $A(t)$:

$$T = T_{max} \times f(\phi) \times h(\dot{\phi}) \times A(t). \tag{1}$$

T_{max} should be proportional to the cross-sectional area of muscles across the joint. Since this simple leg model also accounts for the effects of ankle and hip motion, accurately estimating T_{max} from all the corresponding muscles seems unfeasible. Rather $T_{max} = 2.8 m_d g l$ was chosen by trial and error to generally match with subjects' jump height around their preferred fulcrum numbers (3.5 and 4). Measured isometric angle-torque dependence (Wessel, 1996), $f(\phi)$, at three knee angles (60°, 90°, and 120°) for healthy subjects was augmented for smaller and larger angles (Table 2) and interpolated with cubic splines (Press, 1997). Angular velocity dependence is

$$h(\dot{\phi}) = (\dot{\phi}_{max} - \dot{\phi})/(\dot{\phi}_{max} + G\dot{\phi}), \tag{2}$$

where $\dot{\phi}_{max} = 8\sqrt{g/l}$ is maximum knee angular velocity and $G = 3$ is a constant shape factor. As was explained by Alexander (1990), peak knee angular velocity for standing jumping is close to $4\sqrt{g/l}$, and under unloaded conditions the value should be even larger, yielding the choice of higher $\dot{\phi}_{max}$. Rigid-surface jumping has been found to be relatively insensitive to change of G (Alexander, 1990). Eq. (2) approximates the force–velocity relation of all the corresponding muscles. To account for the increased muscle force during eccentric contraction, $h(\dot{\phi})$ can increase to a saturation value of 1.5 when $(\dot{\phi})$ is negative (flexing) (Selbie & Caldwell, 1996). Eqs. (1) and (2) are a more complex version of Alexander's knee-torque model.

Table 2
Knee angle-torque dependence $f(\phi)$ at different angles

ϕ (deg)	0	30	60	90	120	150	180
$f(\phi)$	0	0.3973	0.6994	0.9061	0.9897	0.7098	0.0470

The function $A(t)$ is approximated by a cubic-spline fit of nodal activation values $A(t^*)$ at 10 times t^* throughout contact. These nodes are the control variables whose optimal values maximize jump height. Moreover, $A(t)$ models the effect of all muscles crossing the knee, but the same activation/deactivation timing for every muscle is not expected. Thus the typical first-order time constant approximation for a single muscle is not adopted. The rate of change of $A(t)$ is rather a free value bounded by the mean of muscle activation and deactivation time constants, typically 20 and 200 ms (Pandy et al., 1990). Therefore, $|dA(t)/dt| \leqslant 1/0.11 \text{ s}^{-1}$. The same approach has been adopted and validated in baseball pitching simulations (Fujii & Hubbard, 2002). $A(t)$ ranges from 0 (relaxed) to +1 (fully activated). Although flexion is possible, $A(t) \geqslant 0$ because the jumper cannot pull up on the surface.

Since the leg is assumed massless, it must be in equilibrium, so that the jumper–surface interaction force $F = T/(l \cos \frac{\phi}{2})$. Board acceleration arises from the spring and jumper contact forces and gravity, while the jumper experiences only the contact force and gravity. Equations of motion for the two mechanical degrees of freedom are written by summing forces in the vertical direction and applying Newton's second law:

$$\begin{cases} \ddot{x}_b = -(x_b \times k/m_b + F/m_b + g), \\ \ddot{x}_d = F/m_d - g. \end{cases} \tag{3}$$

The state vector $[x_b; x_d; \dot{x}_b; \dot{x}_d]$ includes board-tip position x_b and diver c.m. position x_d, measured relative to the spring unstretched position, and their derivatives. Therefore, the initial equilibrium position is $x_b = -(m_d + m_b)g/k$. Since our experimental data showed an averaged knee angle to be around 170° prior to movement, initial knee angle ϕ_i is assumed 170° and initial diver position is $x_d = 2l \sin(\phi_i) - (m_d + m_b)g/k$. Both initial velocities are assumed zero. Takeoff occurs when F vanishes while the diver has an upward velocity.

Since different knee-torque patterns (actually nodal torque activation values) cause different takeoff times, this is an open final time problem and the final time t_f is also one of the control variables (Bryson, 1999). The control goal is to maximize jump height given by

$$J_0 = (x_{df} + v_{df}^2/2g), \tag{4}$$

where x_{df} and v_{df} are takeoff position and velocity.

Maximizing (4) is subject to state and control constraints. The constraint $x_d - x_b < 2l$ implies $\phi < 180°$. Minimum knee angle is also constrained arbitrarily by $\phi_{min} \geqslant 90°$ because angles less than this rarely, if ever, occur in practice. Sensitivity to this constraint is studied using $\phi_{min} \geqslant 60°$. Due to the massless-leg assumption, the board can oscillate almost freely with large amplitude which helps storing potential energy. Simulated minimum knee angle can be unrealistically small without this constraint. In optimal knee-torque activation calculations, nodal activation is not constrained formally. Rather $A(t)$ is truncated when it lies outside [0, 1]. Experimental data show that maximal board depression duration is about 0.5 s, so the terminal

time is constrained $t_f \leqslant 1.5$ s since longer duration may result in "excessive" knee flexion/extension oscillations before takeoff. This is not allowed by the rules (NCAA, 2001) which state that "the diver must not rock the board excessively or lift their feet from the board before takeoff."

Whenever constraints are violated, a penalty function is subtracted from the objective function J_0 to give the new objective function (Reklaitis, Ravindran, & Ragsdell, 1983):

$$J = J_0 - \sum_i c_i p_i, \tag{5}$$

where p_i is the square of the constraint violation and c_i is a weighting coefficient chosen arbitrarily to be 10^5. Thus the problem becomes an unconstrained maximization, where possible violations of the constraints decrease the value of the objective function.

To reduce computational effort, only 10 nodes are needed to represent the activation function since doubling the number increases jump height by less than 0.2 cm. These nodes are equally spaced throughout contact with the first at $t = 0$ and the last at takeoff. The symbolic dynamics software AUTOLEV (Schaechter, Levinson, & Kane, 1996) was used to derive the equations of motion and code them into a C program. The integration routine employs Kutta–Merson algorithm (Fox, 1962) with 10^{-8} and 10^{-7} as the absolute and relative error tolerance, respectively. After joint torque and optimization routines were included, the program was run on a personal computer (with Intel Pentium IV processor). To maximize the likelihood of finding the global rather than a local maximum, a genetic algorithm (Belegundu & Chandrupatla, 1999) was used first. Combined with the downhill simplex method (Press, 1997), optimal solutions were found more confidently.

Simulation results are compared to jumping experiments conducted on a Maxiflex "B" springboard. One male ($m_d = 84.0$ kg; $l = 0.47$ m) diver and one female ($m_d = 44.0$ kg; $l = 0.39$ m) diver, both with about one year of experience, reported preferred standing dive fulcrum settings $S = 3.5$ and 4, respectively. Although kinematic results are presented for only one fulcrum setting, we believe these are typical of jumps at other fulcrum settings. After their informed consent and approval by the University Human Subjects Research Review Committee was obtained, they performed two maximal-height backward standing jumps onto a mat at $S = 1$, 5, and 9 and, to eliminate arm-motion effects, jumped with arms against the chest. Three high-speed cameras (240 Hz) and a motion analysis (Motion Analysis, Eva 7.0, Santa Rosa, CA) system recorded and determined positions of six reflective markers at the board tip, fifth metatarsal, ankle, knee, hip, and shoulder.

3. Results

Experimental results are included for general comparison but not for exactly matching with simulation because jumpers might not perform optimally and because of the model's simplicity. Simulated results agree reasonably well with experiments

except for minor discrepancies. A simulated optimal male diving jump ($S = 5$, $T_{max} = 2.8m_d gl$, $\phi_{min} \geqslant 90°$), denoted S90, and experimental results at the same fulcrum setting are compared (Fig. 2). For the actual jump, it is hard to determine start timing due to small oscillations caused by ankle movement prior to knee flexion. Thus we arbitrarily set the takeoff time $t_f = 0$, and use the simulated duration to specify the start time. Table 3 compares certain features of S90 and the average of two actual jumps. The knee angle constraint is active during maximal knee flexion. The largest discrepancies between simulated and measured results are in the board tip and knee angle kinematics early in the contact period. Possible reasons for discrepancies are addressed in Section 4.

Both optimal simulated and measured results (across different fulcrum settings) suggest a general movement pattern for achieving maximum height and show clearly that the strategy is different from rigid-surface jumping strategies. All simulations show partial knee flexion followed by maximal flexion and partial knee-torque activation followed by maximal activation. This strategy corresponds to real divers rocking the board with the ankle before maximally pressing the board. Contrary to jumping on a rigid surface, the activation level at takeoff vanishes (Fig. 2c) instead of remaining at maximal activation (Selbie & Caldwell, 1996).

Simulations with the constraint $\phi_{min} \geqslant 90°$ (S90) suggest a specific maximum-height fulcrum setting for divers (Fig. 3), and seem to agree with the shape of the measured height–fulcrum relation. Both the male and female models predict highest jumps at $S = 3$, while the limited experimental data shows that the male jumps highest at $S = 5$ and the female jumps highest at $S = 1$. However, there is larger difference in the jump height at $S = 9$ for both jumpers. To test the sensitivity of the optimal height–fulcrum relation to the knee angle constraint, simulations were also performed with $\phi_{min} \geqslant 60°$ (S60) and T_{max} was adjusted to $2m_d gl$ (in the same way as $2.8m_d gl$ was chosen previously) to generally match with measured height. Jump height of S60 increases with increasing fulcrum number (Fig. 3). Contact time increases with S for all simulated cases, and contact durations in S60 are longer than those in S90, probably due to larger knee range of motion (Fig. 4).

Comparison of male and female jump height confirms the hypothesis that jump height depends on body size/strength (Fig. 3). We also simulated jumps with different mass and leg length. Table 4 shows jump height vs. S with $T_{max} = 2m_d gl$ and $\phi_{min} \geqslant 60°$ for nominal and reduced m_d (84 and 70 kg) and nominal l (0.47 m). Table 5 shows jump height vs. S with $T_{max} \geqslant 2.8m_d gl$ and $\phi_{min} \geqslant 90°$ for nominal and increased l (0.47 and 0.53 m) and nominal m_d (84 kg). With the assumption that maximum strength is proportional to the product of mass and length, decreasing mass alone by 17% decreases jump height by less than 2.8 cm and the fulcrum–jump height relation remains relatively unchanged (Table 4). However, changing leg length has a stronger effect on jump height and changes the shape of the fulcrum–jump height relation. Decreasing leg length alone by 17% decreases jump height from 10 to 13 cm and the optimal S shifts from 3 to 1 (Fig. 3 and Table 5). On the other hand, strength alone has the strongest effect on jump height. Decreasing the maximum knee torque by 17% decreases jump height by 12–14 cm for all fulcrum settings, but takeoff time and fulcrum–jump height relations remain essentially unchanged.
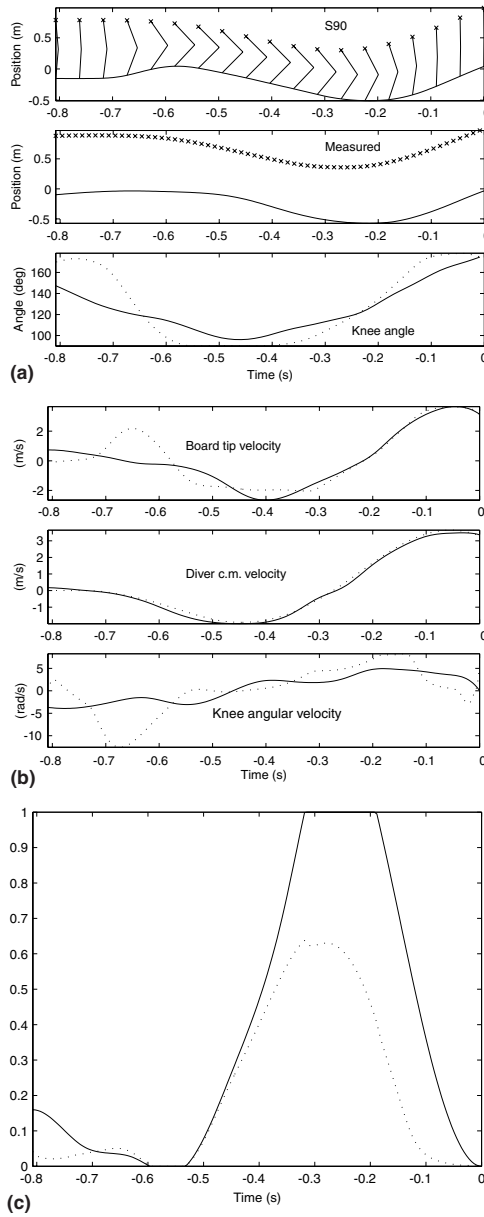
Fig. 2. (a) Simulated optimal jumps with constraint $\phi_{\min} \geqslant 90°$ (S90) and measured jumps at fulcrum setting = 5; board tip (—) and diver c.m. (×) position vs. time. Knee angle for simulation (···) and measured results (—) are also plotted. (b) Board tip velocity, diver c.m. velocity, and knee angular velocity vs. time; simulated S90 (···) and measured jumps (—). (c) Optimal simulated (S90) knee activation (—) and knee torque (···) vs. time. Knee torque is normalized by dividing its value by maximum isometric torque. Activation pattern consists of partial activation followed by maximal activation.

Table 3
Features of simulated S90, and actual jumps shown in Fig. 2

	Actual	S90
Maximum board depression (m)	0.571	0.508
Minimum jumper c.m. velocity (m/s)	−1.993	−1.913
Jumper vertical takeoff c.m. velocity (m/s)	3.356	3.313
Maximum jumper c.m. flight height (m)	1.550	1.540
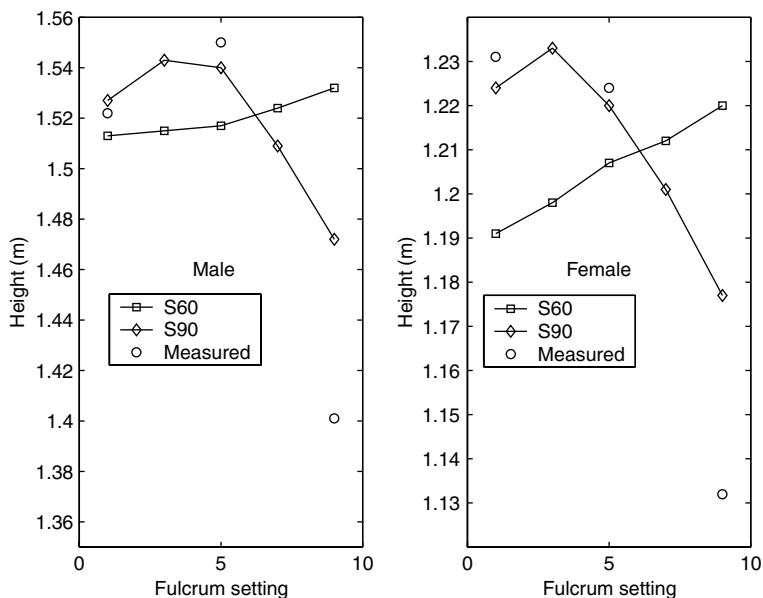
Fig. 3. Simulated and measured male and female jump height vs. fulcrum setting S. Range of motion constraints affect the dependence of optimal height on fulcrum setting.

4. Discussion

The general agreement between simulated and measured results shows the ability of the extremely simple model to make reasonable predictions of jumper c.m. velocity, in spite of the fact that it cannot exactly reproduce the entire diver–board interaction kinematics. Although we suspect the discrepancies in larger board tip and knee angular velocities early in the contact period are due to the lack of leg mass, our preliminary four-segment springboard jumping study (with leg mass) also shows similar results. This means that the theoretically optimal strategy of relaxing the knee before maximum depression (Fig. 2c) inevitably causes larger board tip upward velocity. In addition, since the initial velocities of both the real jumper and board tip are not zero due to ankle movement (Fig. 2b), exact matching with measurement is not expected.
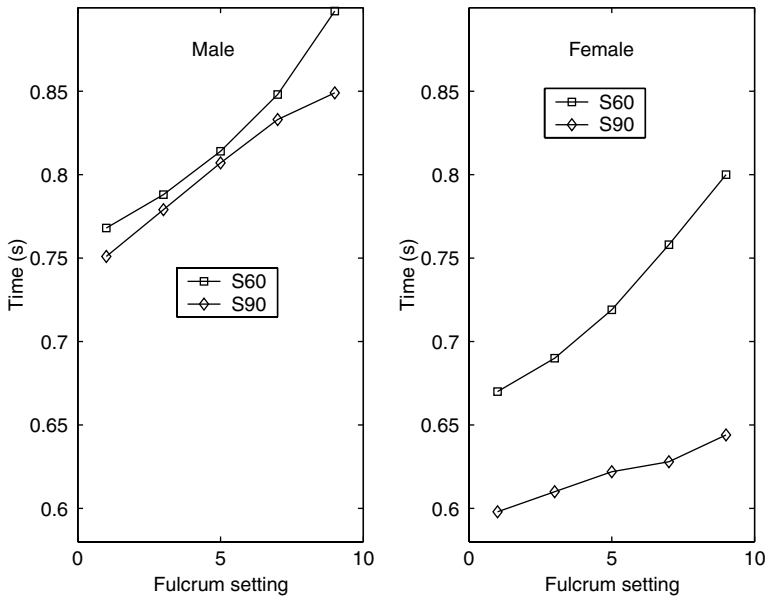
Fig. 4. Simulated male and female contact time vs. fulcrum setting S. Contact durations in S60 are longer than those in S90.

Table 4
Effect of diver mass on jump height and contact time vs. fulcrum with constraint $\phi_{\min} \geqslant 60°$, $T_{\max} = 2m_d gl$, and nominal l (0.47 m). Decreasing mass alone slightly decreases jump height

	Fulcrum				
	1	3	5	7	9
Height (*m*)					
$m_d = 84$ kg (nominal)	1.513	1.515	1.517	1.524	1.532
$m_d = 70$ kg	1.485	1.493	1.503	1.515	1.527
Contact time (*s*)					
$m_d = 84$ kg (nominal)	0.768	0.788	0.814	0.848	0.898
$m_d = 70$ kg	0.731	0.749	0.767	0.801	0.848

In all simulations the jumper's optimal activation pattern consists of two pulses (e.g. Fig. 2). The model first partially activates the knee torque and then relaxes and falls unsupported inducing initial board oscillation. Thereafter the oscillation is amplified using essentially maximal knee activation. In spite of these board oscillations, the jumper's velocity is negative until about 0.3 s before takeoff. This movement strategy is found for all S90 jumps.

Why should the optimal diver strategy consist of only partial knee activation during the first pulse? To utilize the springboard effectively, a diver needs to give

Table 5
Effect of leg length on jump height and contact time vs. fulcrum with constraint $\phi_{\min} \geqslant 90°$, $T_{\max} = 2.8m_{\mathrm{d}}gl$, and nominal m_{d} (84 kg). The change in leg length from nominal is subtracted from jump height for a better comparison. Increasing leg length alone substantially increases jump height.

	Fulcrum				
	1	3	5	7	9
Height (m)					
$l = 0.39$ m	1.431	1.430	1.415	1.392	1.357
$l = 0.47$ m (nominal)	1.527	1.543	1.540	1.509	1.472
$l = 0.53$ m	1.592	1.605	1.611	1.597	1.576
Contact time (s)					
$l = 0.39$ m	0.742	0.761	0.788	0.810	0.835
$l = 0.47$ m (nominal)	0.751	0.779	0.807	0.833	0.849
$l = 0.53$ m	0.772	0.798	0.821	0.841	0.862

the board some initial momentum by pressing the board. But too large a knee torque would cause the diver's feet to leave the board. Therefore, the best strategy is first to activate joint torque partially followed by maximal activation. The knee gradually relaxes from the initial activation level because more rapid decrease of activation causes larger board oscillations which lead to smaller knee angles that violate the constraint $\phi_{\min} \geqslant 90°$. Minimum knee angle occurs when the board is at the highest point where maximum energy can be stored before board depression. Measured data shows that minimum knee angle occurs about 0.15 s after maximum board rebound.

Differences in torque activation strategies between rigid and compliant-surface jumping arise from the additional surface motion degree of freedom. In the former, maximally activated joint torques cause maximum joint angular velocity that leads to zero ground force (according to the force–velocity curve) for takeoff and maximal jump height is achieved. In the latter, however, maximal activation and joint torque are timed to occur around maximal board deflection when the board is best able to resist. Timing maximum knee torque too early or late does not allow as much work to be stored in useable takeoff kinetic energy. Moreover, in rigid-surface jumping, takeoff occurs before reaching a straight posture (Selbie & Caldwell, 1996) and joint extension continues after takeoff. But in springboard jumping takeoff occurs with the leg nearly straight, which is required to ''ride'' the board just before takeoff, simultaneously extracting as much of its energy as possible and maximizing the c.m. height at takeoff.

The fulcrum–height relation in S90 suggests a theoretically optimal fulcrum setting for maximizing jump height (Fig. 3). Predicted jump height agrees with our experiments at low fulcrum settings ($S <= 5$) but not well at $S = 9$. We believe this may be due to the fact that the experimental subjects' preferred fulcrum settings ($S = 3.5$ and 4) prevented expertise in optimizing jump height at $S = 9$. Since the real springboard deflection angle at the tip can be as big as 60° at large fulcrum settings,

difficulty in gripping the board probably also decreases the performance. Moreover, it was suggested that longer contact time reduces the storage and recovery of elastic energy of the legs (Farley, Blickhan, Saito, & Taylor, 1991). However, the result that jump height increases with increasing fulcrum number in S60 also agrees with previous predictions. Boda (1993) argued that if a diver could relax and wait for the springboard, the looser setting (higher fulcrum number) might result in more height. Jones and Miller (1996) stated that theoretically larger vertical velocity can be generated using larger S.

The surprising difference in the fulcrum–height relation between the S60 and S90 results is undoubtedly due to the difference in joint range-of-motion. With a smaller range-of-motion in S90 ($90 \leqslant \phi \leqslant 180°$), the jumper may not be able to initiate board oscillation and load the board as effectively. Therefore, less energy is stored in the board spring and larger isometric knee torque is needed to give reasonable takeoff velocity. A softer board needs more depression than a stiffer board to store the same amount of elastic energy. Therefore, a soft board is not favorable for small ranges of motion. This argument was tested by using a longer leg (0.53 m) in S90 to increase the possible vertical displacement of the (virtual) foot and the jump height increased up to $S = 5$ (Table 5).

Maximum-height fulcrum settings may not be the preferred ones. Boda (1993) found that preferred fulcrum settings in standing dives differ from the actual fulcrum settings that generate maximum height. Optimal fulcrum setting was identified as a function of preferred fulcrum setting, frequency of oscillation on the ground, and diver weight. His optimal fulcrum setting (around 4) is similar to our measured data and S90 male model results. As Boda explained, larger fulcrum settings may cause body leaning and result in less vertical velocity at takeoff. Although our simple model allows only vertical motion, the S90 results explain smaller jump height at higher fulcrum settings by insufficient board depression. However, since the constraint $\phi_{\min} \geqslant 90°$ is added to the model artificially, use of a more complex multi-link model to better understand the mechanism will be the subject of future work.

5. Conclusions

An extremely simple model for standing springboard dives predicts optimal jumping strategies that maximize height. These consist of a double pulse pattern, the first and last of which are partially and fully active, respectively. Similar knee-torque activation patterns are found for all jumper sizes and fulcrum settings and are different from those in jumping from a rigid surface. Simulation results agree reasonably with experimental results except for board tip and knee kinematics early in the board contact period. With the constraint on knee range-of-motion, the model is able to predict a jump height vs. fulcrum relation similar to experiments. With a larger allowed knee range-of-motion, jump height increases with board compliance. Achievable height increases with jumper leg length, mass, and more effectively, strength.

References

Alexander, R. M. (1990). Optimum takeoff techniques for high and long jumps. *Philosophical Transactions of the Royal Society of London B, 329*, 3–10.

Belegundu, A. D., & Chandrupatla, T. R. (1999). *Optimization Concepts and Applications in Engineering*. Upper Saddle River, NJ: Prentice Hall.

Bobbert, M. F., & van Ingen Schenau, G. J. (1988). Coordination in vertical jumping. *Journal of Biomechanics, 21*, 249–262.

Boda, W. L. (1993). Predicting optimal fulcrum setting for backward takeoffs. In US Diving Sport Science Seminar 1993 Proceedings (pp. 60–66).

Bryson, A. E. (1999). *Dynamic optimization*. Menlo Park, CA: Addison-Wesley.

Challis, J. H. (1998). An investigation of the influence of bi-lateral deficit on human jumping. *Human Movement Science, 17*, 307–325.

Farley, C. T., Blickhan, R., Saito, J., & Taylor, R. (1991). Hopping frequency in humans: A test of how springs set stride frequency in bouncing gaits. *Journal of Applied Physiology, 71*, 2127–2132.

Ferris, D. P., & Farley, C. T. (1997). Interaction of leg stiffness and surface stiffness during human hopping. *Journal of Applied Physiology, 82*, 15–22.

Fox, L. (1962). *Numerical solutions of ordinary and partial differential equations*. Palo Alto: Addison-Wesley.

Fujii, N., & Hubbard, M. (2002). Validation of a three-dimensional baseball pitching model. *Journal of Applied Biomechanics, 18*, 135–154.

Jones, I. C., & Miller, D. I. (1996). Influence of fulcrum position on springboard response and takeoff performance in the running approach. *Journal of Applied Biomechanics, 12*, 383–408.

Jones, I. C., Pizzimenti, M. P., & Miller, D. I. (1993). A springboard feedback system: Considerations and implications for coaching. In R. Malina & J. L. Gabriel (Eds.), *U.S. Diving Sport Science Seminar 1993 Proceedings* (pp. 67–79). Indianapolis: US Diving Publications.

Kooi, B. W., & Kuipers, M. (1994). The dynamics of springboard. *International Journal of Sport Biomechanics, 10*, 335–351.

Levine, W. S., Christodoulou, M., & Zajac, F. E. (1983). On propelling a rod to a maximum vertical or horizontal distance. *Automatica, 19*, 321–324.

Levine, W. S., Zajac, F. E., Belzer, M. R., & Zomlefer, M. R. (1983). Ankle controls that produce a maximal vertical jump when other joints are locked. *IEEE Transactions on Automatic Control, 11*, 1008–1016.

McMahon, T. A. (1978). Fast running tracks. *Scientific American, 239*, 148–163.

McMahon, T. A., & Greene, P. R. (1979). The influence of track compliance on running. *Journal of Biomechanics, 12*, 893–904.

Miller, D. I. (1983). Springboard reaction torque patterns during non-twisting dive takeoffs. In H. Matsui & K. Kobayashi (Eds.), *Biomechanics VIII-B* (pp. 822–827). Champaign, IL: Human Kinetics.

Miller, D. I., & Munro, C. F. (1984). Body segment contributions to height achieved during the flight of a springboard dive. *Medicine and Science in Sport and Exercise, 16*(3), 234–242.

Miller, D. I., & Munro, C. F. (1985). Greg Louganis' springboard takeoff: I. temporal and joint position analysis. *International Journal of Sport Biomechanics, 1*, 209–220.

Miller, D. I., Osborne, M. J., & Jones, I. C. (1998). Springboard oscillation during hurdle flight. *Journal of Sports Sciences, 16*, 571–583.

Miller, D. I., & Sprigings, E. J. (2001). Factors influencing the performance of springboard dives of increasing difficulty. *Journal of Applied Biomechanics, 17*, 217–231.

NCAA, (2001). *2002 NCAA Men's and women's swimming and diving rules*. National College Athletic Association. Retrieved April 30, 2003, from www.ncaa.org/library/rules/2002/2002_swim_dive_rules.pdf.

Pandy, M. G., Zajac, F. E., Sim, E., & Levine, W. S. (1990). An optimal control model for maximum-height human jumping. *Journal of Biomechanics, 23*, 1185–1198.

Press, W. H. (1997). *Numerical recipes in C: The art of scientific computing* (2nd ed.). New York: Cambridge University Press, Retrieved April 30, 2003, from http://www.ulib.org/webRoot/Books/Numerical_Recipes/bookcpdf.html.

Reklaitis, G. V., Ravindran, A., & Ragsdell, K. M. (1983). *Engineering optimization: Methods and applications*. New York: Wiley.

Sanders, R. H., & Wilson, B. D. (1987). Angular momentum requirements of the twisting nontwisting forward 1-somersault dive. *International Journal of Sport Biomechanics, 3*, 47–62.

Schaechter, D. B., Levinson, D. A., Kane, T. R. (1996). AUTOLEV (Version 3).

Selbie, W. S., & Caldwell, G. E. (1996). A simulation study of vertical jumping from different starting postures. *Journal of Biomechanics, 29*, 1137–1146.

Seyfarth, A., Blickhan, R., & van Leeuwen, J. L. (2000). Optimum takeoff techniques and muscle design for long jump. *Journal of Experimental Biology, 203*, 741–750.

Seyfarth, A., Friedrichs, A., Wank, V., & Blickhan, R. (1999). Dynamics of the long jump. *Journal of Biomechanics, 32*, 1259–1267.

van Soest, A. J., Schwab, A. L., Bobbert, M. F., & van Ingen Schenau, G. J. (1993). The influence of the biarticularity of the gastrocnemius muscle on vertical-jumping achievement. *Journal of Biomechanics, 26*, 1–8.

Sprigings, E. J., Stilling, D. S., & Watson, L. G. (1989). Development of a model to represent an aluminum springboard in diving. *International Journal of Sport Biomechanics, 5*, 297–307.

Sprigings, E. J., Stilling, D. S., Watson, L. G., & Dorotich, P. D. (1990). Measurement of the modeling parameters for a Maxiflex "B" springboard. *International Journal of Sport Biomechanics, 6*, 325–335.

Sprigings, E. J., & Watson, L. G. (1983). A mathematical search for the optimal timing of the armswing during springboard diving takeoffs. In D. A. Winter et al. (Eds.), *Proceedings of Ninth International Congress of Biomechanics*BIOMECHANICS IX-B (pp. 389–394). Champaign, IL: Human Kinetics.

Wessel, J. (1996). Isometric strength measurements of knee extensors in women with osteoarthritis of the knee. *Journal of Rheumatology, 23*, 328–331.